

# Development of robust $\bar{X}$ -bar charts with unequal sample sizes

Chanseok Park

Applied Statistics Laboratory  
Department of Industrial Engineering  
Pusan National University  
Busan 46241, Korea

Linhan Ouyang

College of Economics and Management  
Nanjing University of Aeronautics and Astronautics  
Nanjing, Jiangsu 211106, China

Min Wang<sup>†</sup>

Department of Management Science and Statistics  
The University of Texas at San Antonio  
San Antonio, TX, USA

## Abstract

The traditional variable control charts, such as the  $\bar{X}$  chart, are widely used to monitor variation in a process. They have been shown to perform well for monitoring processes under the general assumptions that the observations are normally distributed without data contamination and that the sample sizes from the process are all equal. However, these two assumptions may not be met and satisfied in many practical applications and thus make them potentially limited for widespread application especially in production processes. In this paper, we alleviate this limitation by providing a novel method for constructing the robust  $\bar{X}$  control charts, which can simultaneously deal with both data contamination and unequal sample sizes. The proposed method for the process parameters is optimal in a sense of the best linear unbiased estimation.

---

<sup>†</sup>Corresponding author. Email: [min.wang3@utsa.edu](mailto:min.wang3@utsa.edu)

Numerical results from extensive Monte Carlo simulations and a real data analysis reveal that traditional control charts seriously underperform for monitoring process in the presence of data contamination and are extremely sensitive to even a single contaminated value, while the proposed robust control charts outperform in a manner that is comparable with the traditional ones, whereas they are far superior when the data are contaminated by outliers.

**Keywords:** Average run length; BLUE estimator; relative efficiency; robustness; statistical process control.

## 1 Introduction

Variables control charts provide a powerful tool for monitoring variation in a process where the measurement is a variable (Montgomery, 2013), which can be measured on a continuous scale, such as length, pressure, width, temperature, and volume, in a time-ordered sequence. Since their introduction by Shewhart (1926), variable control charts, such as the Shewhart control chart, have been extensively adopted to detect if a process is in a state of control in different fields including industrial manufacturing, service sectors, and healthcare systems, to name just a few. The statistical control charts can generally be classified into two phases: Phase-I and Phase-II (Vining, 2009; Montgomery, 2013). First, in Phase-I monitoring, we establish reliable control limits with a clean set of process data and in Phase-II analysis, we use the control limits obtained in Phase-I in the monitoring of a process by comparing the statistic for each successive subgroup as future observations are obtained. We refer the interested reader to the collection of textbooks and papers in Montgomery (2013, 2019); Faraz et al. (2019); Woodall and Faltin (2019) for details.

In most Phase II monitoring situations, the majority of variable control charts usually depend on the unknown process parameters that need to be estimated based on an in-control Phase I sample or historical data, indicating the quality of these data plays an important role in determining the performance of the Phase-II control charts. It deserves mentioning that the constructions of traditional control charts and other related techniques for statistical process monitoring usually requires the following two general assumptions: (i) the observations are normally distributed without data contamination (Wheeler, 2010; Khakifirooz et al., 2021) and (ii) the sample sizes from the process are all equal. However, these two assumptions are quite restrictive for developing efficient control charts for monitoring the manufacturing process.

The traditional control charts, such as the  $\bar{X}$  chart, are constructed using the sample mean and standard deviation which are sensitive to data contamination, because their breakdown points are zero. Recently, Yao and Chakraborti (2021) pointed out the importance of accounting for the effect of parameter estimation in the Shewhart-type Phase I chart, since the direct use of the

control charts with inaccurate parameter estimates for process monitoring could increase the rate of false alarms to an unacceptable level and even result in misleading results in practical applications, especially when the Phase I data are contaminated by outliers due to the measurement errors, the volatile operating conditions, among others. To overcome this limitation, researchers developed robust control charts by incorporating robust estimators for the location and scale parameters. For instance, Rocke (1989) obtained the control limits based on the trimmed mean and the interquartile range. Alloway and Raghavachari (1991) and Pappanastos and Adams (1996) used the Hodges-Lehmann control chart for location. Janacek and Meikle (1997) used the median, and Abu-Shawiesh (2008) considered the median absolute deviation (MAD) for constructing robust control charts.

In addition, the construction of traditional control charts often requires the sample sizes to be all equal in the process, whereas this requirement may not be met in practice due to missing observations, cost constraints, etc. As commented by Kim and Reynolds (2005), since the importance of each variable is different, it is necessary to take the variable sample size issue into consideration in the field of statistical process control. To tackle the issue of unbalanced sample sizes, Kosztyán and Katona (2018) proposed a risk-based concept for the design of an  $\bar{X}$  chart with variable sample size, in which the optimal sample size is determined by the genetic algorithm and the Nelder-Mead direct algorithm.

However, to our knowledge, no study has proposed the construction of robust  $\bar{X}$  chart which can simultaneously deal with both data contamination and unequal sample sizes. To fill this gap, we first mitigate the effects of data contamination for the parameter estimation by incorporating robust estimators with high breakdown point values, such as the median and Hodges-Lehmann (HL) estimator for the location parameter and the MAD and Shamos estimators for the scale estimation parameter. To overcome the issue of unequal sample sizes, we take a weighted average approach in calculating  $\bar{X}$  based on the sample sizes, since estimating a parameter from the larger samples is more reliable than that from smaller samples and the weighted average should be used instead of the simple average (Burr, 1969). As an illustration from the location estimation, we assume that there are  $m$  samples (subgroups) and  $n_i$  is the sample size of the  $i$ th sample from a manufacturing process. Then the simple average,  $\bar{\bar{X}}_A = \sum_{i=1}^m \bar{X}_i/m$ , is inferior to the weighted average,  $\bar{\bar{X}}_B = \sum_{i=1}^m n_i \bar{X}_i / \sum_{i=1}^m n_i$ , in a sense that  $\text{Var}(\bar{\bar{X}}_A) \geq \text{Var}(\bar{\bar{X}}_B)$ . Note that  $\bar{\bar{X}}_A$  has an unweighted average of the estimates while  $\bar{\bar{X}}_B$  has a weighted average with weights proportional to the sample sizes. This idea pays off with the sample means. However, for other estimators such as the median and MAD estimators, although it looks appealing to use the weights proportional to the sample sizes, the weights simply proportional to the sample sizes can make the estimation worse as will be shown in Section 2.

The remainder of this paper is organized as follows. In Section 2, we proposed the unbiased location and scale estimators for the process parameters with unequal sample sizes. In Section 3, we carry out simulation studies to investigate the performance of the proposed estimation methods under no data contamination and under data contamination. In Section 4, we briefly introduce how to construct robust control charts with the proposed robust estimators and compare the performance of the robust control charts under consideration. An illustrative example is provided in Section 5 for demonstrative purposes. Finally, several concluding remarks are given in Section 6.

## 2 Process parameter estimation with unequal sample sizes

In this section, we propose the unbiased location and scale estimators for the process parameters under the assumption that each sample has different sample sizes and that the underlying distribution is normally distributed. Let  $X_{ij}$  be the  $i$ th sample (subgroup) of size  $n_i$  from a Phase-I process for  $j = 1, 2, \dots, n_i$  and  $i = 1, 2, \dots, m$ . We assume that  $X_{ij}$ 's are independent and identically distributed (iid) random variables from a normal distribution with location  $\mu$  and variance  $\sigma^2$ .

### 2.1 Estimation of the location parameter

The following location estimators for the population mean parameter are widely used in the quality control literature,

$$\bar{\bar{X}}_A = \frac{\bar{X}_1 + \bar{X}_2 + \dots + \bar{X}_m}{m} = \frac{1}{m} \sum_{i=1}^m \bar{X}_i \quad (1)$$

and

$$\bar{\bar{X}}_B = \frac{n_1 \bar{X}_1 + n_2 \bar{X}_2 + \dots + n_m \bar{X}_m}{n_1 + n_2 + \dots + n_m} = \frac{1}{N} \sum_{i=1}^m n_i \bar{X}_i, \quad (2)$$

where  $\bar{X}_i = \sum_{j=1}^{n_i} X_{ij}/n_i$  and  $N = \sum_{i=1}^m n_i$ ; see, for example, Equations (6.2) and (6.30) of Montgomery (2013) for  $\bar{\bar{X}}_A$  and  $\bar{\bar{X}}_B$ , respectively. Their variances are given by  $\text{Var}(\bar{\bar{X}}_A) = \sigma^2 \sum_{i=1}^m n_i^{-1}/m^2$  and  $\text{Var}(\bar{\bar{X}}_B) = \sigma^2/N$ . Using the inequality of the arithmetic and harmonic means, it can be easily shown that  $\text{Var}(\bar{\bar{X}}_A) \geq \text{Var}(\bar{\bar{X}}_B)$  (Park and Wang, 2020). In this case, the estimator  $\bar{\bar{X}}_B$  is actually optimal in a sense that it is the best linear unbiased estimator (BLUE), which will be shown later.

Analogous to  $\bar{\bar{X}}_A$  in (1) and  $\bar{\bar{X}}_B$  in (2), we can generalize the above with the following location estimators to estimate the population mean parameter  $\mu$ .

$$\bar{\hat{\mu}}_A = \frac{\hat{\mu}_1 + \hat{\mu}_2 + \dots + \hat{\mu}_m}{m} = \frac{1}{m} \sum_{i=1}^m \hat{\mu}_i \quad (3)$$

and

$$\bar{\hat{\mu}}_B = \frac{n_1\hat{\mu}_1 + n_2\hat{\mu}_2 + \cdots + n_m\hat{\mu}_m}{n_1 + n_2 + \cdots + n_m} = \frac{1}{N} \sum_{i=1}^m n_i\hat{\mu}_i, \quad (4)$$

where  $\hat{\mu}_i$  denotes the unbiased location estimator of  $\mu$  with the  $i$ th sample. It can be easily shown that they are unbiased, such that  $E(\bar{\hat{\mu}}_A) = \mu$  and  $E(\bar{\hat{\mu}}_B) = \mu$  and that their variances are given by  $\text{Var}(\bar{\hat{\mu}}_A) = \sum_{i=1}^m V_i/m^2$  and  $\text{Var}(\bar{\hat{\mu}}_B) = \sum_{i=1}^m n_i^2 V_i/N^2$ , where  $V_i = \text{Var}(\hat{\mu}_i)$ .

When the sample mean is considered, it is always true that  $\text{Var}(\bar{X}_A) \geq \text{Var}(\bar{X}_B)$  as aforementioned. However, when other estimators are considered,  $\text{Var}(\bar{\hat{\mu}}_A) \geq \text{Var}(\bar{\hat{\mu}}_B)$  does not hold in general. For example, when the sample median is used with  $n_1 = 4$  and  $n_2 = 5$ , by using numerical results from Park and Wang (2022) and Park et al. (2022), we obtain  $V_1 = \text{Var}(\hat{\mu}_1) = (1.1930/4)\sigma^2 = 0.29825\sigma^2$  and  $V_2 = \text{Var}(\hat{\mu}_2) = (1.4339/5)\sigma^2 = 0.28678\sigma^2$ , indicating that  $\text{Var}(\bar{\hat{\mu}}_A) = 0.146\sigma^2 < \text{Var}(\bar{\hat{\mu}}_B) = 0.147\sigma^2$ . In what follows, we propose the BLUE for the location parameter  $\mu$ .

**Lemma 1.** *The BLUE for the location parameter  $\mu$  is given by*

$$\bar{\hat{\mu}}_C = \frac{\sum_{i=1}^m (\hat{\mu}_i/\nu_i^2)}{\sum_{i=1}^m (1/\nu_i^2)}, \quad (5)$$

where  $\nu_i^2$  is the variance of  $\hat{\mu}_i$  under the standard normal distribution.

*Proof.* We consider a linear estimator in the form of  $\bar{\hat{\mu}}_C = \sum_{i=1}^m w_i\hat{\mu}_i$  where  $E(\hat{\mu}_i) = \mu$  as aforementioned. Since  $\bar{\hat{\mu}}_C$  is unbiased such that  $E(\bar{\hat{\mu}}_C) = \mu$ , we have  $\sum_{i=1}^m w_i = 1$ . Thus, our objective is to minimize  $\text{Var}(\bar{\hat{\mu}}_C) = \sum_{i=1}^m w_i^2 V_i$  with the constraint  $\sum_{i=1}^m w_i = 1$ . We can set up the auxiliary function with the Lagrange multiplier  $\lambda$  given by

$$\Psi = \sum_{i=1}^m w_i^2 V_i - \lambda \left( \sum_{i=1}^m w_i - 1 \right).$$

Differentiating  $\Psi$  with respect to  $w_i$  and setting it to zero, we have  $2w_i V_i - \lambda = 0$ , which results in  $w_i = \lambda/(2V_i)$ . Since  $\sum_{i=1}^m w_i = 1$ , we have  $\sum_{i=1}^m \lambda/(2V_i) = 1$  so that  $\lambda = 2/\sum_{i=1}^m (1/V_i)$ . Then we obtain  $w_i = (1/V_i)/\sum_{i=1}^m (1/V_i)$ . Since the normal distribution is a part of the location-scale family of distributions, we have  $V_i = \sigma^2\nu_i^2$ . Thus, we have  $w_i = (1/\nu_i^2)/\sum_{i=1}^m (1/\nu_i^2)$ , which completes the proof.  $\square$

We can easily show that  $\text{Var}(\bar{\hat{\mu}}_A) \geq \text{Var}(\bar{\hat{\mu}}_C)$  using the inequality of the arithmetic and harmonic means and that  $\text{Var}(\bar{\hat{\mu}}_B) \geq \text{Var}(\bar{\hat{\mu}}_C)$  using the Cauchy-Schwarz inequality, where  $\text{Var}(\bar{\hat{\mu}}_C) = 1/\sum_{i=1}^m (1/V_i)$ . As mentioned above, there is no clear inequality relation between  $\text{Var}(\bar{\hat{\mu}}_A)$  and  $\text{Var}(\bar{\hat{\mu}}_B)$ , unless the sample mean is considered. For the special case of the sample mean  $\hat{\mu}_i = \bar{X}_i$ ,

the above  $\bar{\hat{\mu}}_C$  is the same as  $\bar{\hat{\mu}}_B$ , since  $V_i = \text{Var}(\hat{\mu}_i) = \sigma^2/n_i$ , which implies that  $\bar{X}_B = \sum_{i=1}^m n_i \bar{X}_i/N$  is optimal.

We here develop a robust BLUE location estimator using the median and HL estimators. Let  $X_{ij} = \mu + \sigma Z_{ij}$ , where  $Z_{ij}$  are iid with  $N(0, 1)$ . Let  $\text{median}(X_i) = \text{median}\{X_{i1}, \dots, X_{in_i}\}$ . We have  $\text{median}(X_i) = \mu + \sigma \cdot \text{median}(Z_i)$ , so that  $\text{Var}\{\text{median}(X_i)\} = \sigma^2 \text{Var}\{\text{median}(Z_i)\}$ . The HL estimator is calculated by the median of all pairwise (Walsh) averages of the observations, which is given by

$$\text{HL}(X_i) = \text{median} \left( \frac{X_{ik} + X_{i\ell}}{2} \right).$$

Here the median of all Walsh averages can be calculated for the three cases (Park et al., 2022): (i)  $k < \ell$ , (ii)  $k \leq \ell$ , and (iii)  $\forall(k, \ell)$ , for  $k, \ell = 1, 2, \dots, n_i$ . Thus, we can have three versions as below

$$\begin{aligned} \text{HL1}(X_i) &= \text{median}_{k < \ell} \left( \frac{X_{ik} + X_{i\ell}}{2} \right), \\ \text{HL2}(X_i) &= \text{median}_{k \leq \ell} \left( \frac{X_{ik} + X_{i\ell}}{2} \right), \end{aligned}$$

and

$$\text{HL3}(X_i) = \text{median}_{\forall(k, \ell)} \left( \frac{X_{ik} + X_{i\ell}}{2} \right).$$

It is noteworthy that all three versions are asymptotically equivalent (Serfling, 2011). In this paper, we use HL1, denoted as HL for brevity. For the HL case, we also have

$$\text{HL}(X_i) = \text{median}_{k < \ell} \left( \frac{X_{ik} + X_{i\ell}}{2} \right) = \mu + \sigma \cdot \text{median}_{k < \ell} \left( \frac{Z_{ik} + Z_{i\ell}}{2} \right) = \mu + \sigma \cdot \text{HL}(Z_i).$$

Thus, we have

$$\text{Var}\{\text{HL}(X_i)\} = \sigma^2 \cdot \text{Var}\{\text{HL}(Z_i)\}.$$

By using the empirical variances of the sample median and HL estimator from Park and Wang (2022) and Park et al. (2022) along with Lemma 1, we can easily obtain the robust BLUE estimators for the population mean based on the sample median and the HL estimator.

## 2.2 Estimation of the scale parameter

Park and Wang (2020) proposed the following unbiased estimators for the population scale  $\sigma$ , which are given by

$$\bar{S}_A = \frac{S_1/c_4(n_1) + S_2/c_4(n_2) + \dots + S_m/c_4(n_m)}{m} = \frac{1}{m} \sum_{i=1}^m \frac{S_i}{c_4(n_i)}, \quad (6)$$

and

$$\bar{S}_B = \frac{S_1 + S_2 + \cdots + S_m}{c_4(n_1) + c_4(n_2) + \cdots + c_4(n_m)} = \frac{\sum_{i=1}^m S_i}{\sum_{i=1}^m c_4(n_i)}, \quad (7)$$

where  $S_i^2 = \sum_{j=1}^{n_i} (X_{ij} - \bar{X}_i)^2 / (n_i - 1)$  and  $c_4(n_i) = \sqrt{2/(n_i - 1)} \cdot \Gamma(n_i/2) / \Gamma((n_i - 1)/2)$ . In a similar way as done above, we can consider the following estimators for the scale parameter given by

$$\bar{\sigma}_A = \frac{\hat{\sigma}_1/C_1 + \hat{\sigma}_2/C_2 + \cdots + \hat{\sigma}_m/C_m}{m} = \frac{1}{m} \sum_{i=1}^m \frac{\hat{\sigma}_i}{C_i}, \quad (8)$$

and

$$\bar{\sigma}_B = \frac{\hat{\sigma}_1 + \hat{\sigma}_2 + \cdots + \hat{\sigma}_m}{C_1 + C_2 + \cdots + C_m} = \frac{\sum_{i=1}^m \hat{\sigma}_i}{\sum_{i=1}^m C_i}, \quad (9)$$

where  $\hat{\sigma}_i$  denotes the estimator of  $\sigma$  with the  $i$ th sample and  $C_i = E(\hat{\sigma}_i)/\sigma$ . Then both  $\bar{\sigma}_A$  and  $\bar{\sigma}_B$  are unbiased. The variances of  $\bar{\sigma}_A$  and  $\bar{\sigma}_B$  are given by

$$\text{Var}(\bar{\sigma}_A) = \frac{1}{m^2} \sum_{i=1}^m \frac{V_i}{C_i^2} \quad \text{and} \quad \text{Var}(\bar{\sigma}_B) = \frac{\sum_{i=1}^m V_i}{(\sum_{i=1}^m C_i)^2},$$

where  $V_i = \text{Var}(\hat{\sigma}_i)$ . We observe from Park and Wang (2020) that  $\text{Var}(\bar{S}_A) \geq \text{Var}(\bar{S}_B)$  using the Chebyshev's sum inequality along with the property that  $c_4(x)$  is increasing and  $1/c_4(x)^2 - 1$  is decreasing.

However, the inequality of  $\text{Var}(\bar{\sigma}_A) \geq \text{Var}(\bar{\sigma}_B)$  does not hold in general. As an illustration, we consider the MAD given by

$$\text{MAD}(X_i) = \frac{\text{median}_{1 \leq j \leq n_i} |X_{ij} - \tilde{\mu}_i|}{\Phi^{-1}(3/4)},$$

where  $\tilde{\mu}_i = \text{median}(X_i)$ . Here  $\Phi^{-1}(3/4)$  is needed to make this estimator Fisher-consistent (Fisher, 1922) for the standard deviation  $\sigma$  under the normal distribution. Since this MAD is not unbiased with a finite sample size, Park and Wang (2022) and Park et al. (2022) obtained the empirical unbiasing factor, denoted by  $c_5(n_i)$ , for this MAD. Thus, we can obtain the *unbiased* MAD with a finite sample size for the standard deviation  $\sigma$  under the normal distribution which is

$$\frac{\text{MAD}(X_i)}{c_5(n_i)}. \quad (10)$$

For example, when the unbiased MAD is used with the sample sizes  $n_1 = 4$  and  $n_2 = 5$ , we have  $\text{Var}(\bar{\sigma}_A) = 0.167\sigma^2$  and  $\text{Var}(\bar{\sigma}_B) = 0.168\sigma^2$  so that we have  $\text{Var}(\bar{\sigma}_A) < \text{Var}(\bar{\sigma}_B)$  in this case.

The term  $c_4(x)$  is the unbiasing factor for the standard deviation and  $1 - c_4(x)^2$  is the variance of the standard deviation under the standard normal distribution. Then we have  $\text{Var}(S/c_4(n)) = \sigma^2(1 - c_4(x)^2)/c_4(x)^2$ . Thus,  $1/c_4(x)^2 - 1 = (1 - c_4(x)^2)/c_4(x)^2$  can be thought of as the ratio of the

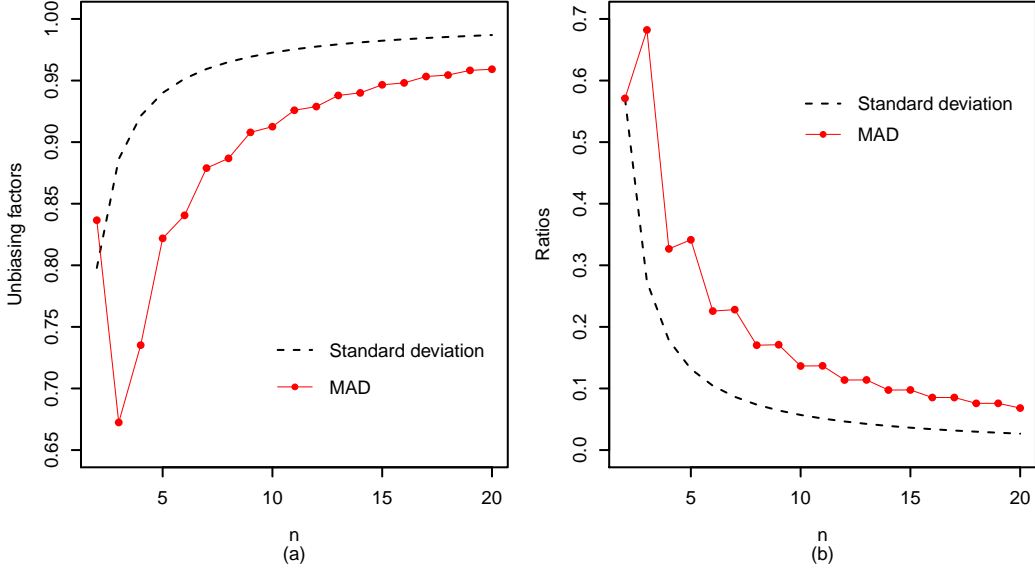


Figure 1: The unbiasing factors and ratios of the squared unbiasing factor to the variance.

variance to the squared unbiasing factor for the estimator under the standard normal distribution. In Figure 1, we draw the unbiasing factors and the ratios of the variance to the squared unbiasing factor for the standard deviation and the unbiased MAD under the standard normal distribution. This figure indicates that the inequality of  $\text{Var}(\bar{\sigma}_A) \geq \text{Var}(\bar{\sigma}_B)$  may not hold for the unbiased MAD. In what follows, we propose the BLUE for the scale parameter.

**Lemma 2.** *The BLUE for the scale parameter is given by*

$$\bar{\sigma}_C = \frac{\sum_{i=1}^m (\gamma_i / \tau_i^2) \hat{\sigma}_i}{\sum_{i=1}^m (\gamma_i^2 / \tau_i^2)}, \quad (11)$$

where  $\gamma_i$  and  $\tau_i^2$  are the expectation and variance of  $\hat{\sigma}_i$  under the standard normal distribution, respectively.

*Proof.* We consider a linear estimator in the form of  $\bar{\sigma}_C = \sum_{i=1}^m w_i \hat{\sigma}_i$ . Since  $E(\bar{\sigma}_C) = \sigma$ , we have  $\sum_{i=1}^m w_i C_i = 1$ , where  $C_i = E(\hat{\sigma}_i) / \sigma$  as mentioned above. With the constraint  $\sum_{i=1}^m w_i C_i = 1$ , the estimator  $\bar{\sigma}_C$  is guaranteed to be unbiased. Thus, our objective is to minimize  $\text{Var}(\bar{\sigma}_C) = \sum_{i=1}^m w_i^2 V_i$  with this constraint, where  $V_i = \text{Var}(\hat{\sigma}_i)$ . We set up the auxiliary function with the Lagrange multiplier  $\lambda$  given by

$$\Psi = \sum_{i=1}^m w_i^2 V_i - \lambda \left( \sum_{i=1}^m w_i C_i - 1 \right).$$

Differentiating  $\Psi$  with respect to  $w_i$  and setting it to zero, we have  $2w_i V_i - \lambda C_i = 0$ , which results in  $w_i = \lambda C_i / (2V_i)$ . Since  $\sum_{i=1}^m w_i C_i = 1$ , we have  $\sum_{i=1}^m \lambda C_i^2 / (2V_i) = 1$  so that  $\lambda = 2 / \sum_{i=1}^m (C_i^2 / V_i)$ . Thus, we have  $w_i = (C_i / V_i) / \sum_{i=1}^m (C_i^2 / V_i)$ . Since the normal distribution is a part of the location-scale family, we have  $C_i = \gamma_i$  and  $V_i = \sigma^2 \tau_i^2$ , so that we have  $w_i = (\gamma_i / \tau_i^2) / \sum_{i=1}^m (\gamma_i^2 / \tau_i^2)$ , which completes the proof.  $\square$



The term  $\gamma_i$  in Lemma 2 can be regarded as an unbiasing factor for  $\hat{\sigma}_i$ . Thus, if  $\hat{\sigma}_i$  is an unbiased estimator of  $\sigma$ , then we have  $\gamma_i = 1$ . Thus, we can rewrite (11) as

$$\bar{\sigma}_C = \frac{\sum_{i=1}^m (1/\tau_i^2) \hat{\sigma}_i}{\sum_{i=1}^m (1/\tau_i^2)}. \quad (12)$$

When  $X_{ij} = \mu + \sigma Z_{ij}$ , we have  $\text{MAD}(X_i) = \sigma \text{MAD}(Z_i)$ . We can then incorporate Lemma 2 into  $\text{MAD}(X_i)$ . We also consider another robust scale estimator called Shamos estimator which is given by

$$\text{Shamos}(X_i) = \frac{\text{median}_{k < \ell} (|X_{ik} - X_{i\ell}|)}{\sqrt{2} \Phi^{-1}(3/4)},$$

which is also biased with a finite sample size. Here  $\sqrt{2} \Phi^{-1}(3/4)$  is needed to make this estimator Fisher-consistent for the standard deviation  $\sigma$  under the normal distribution (Lèvy-Leduc et al., 2011). To make it unbiased with a finite sample, we adopt the empirical unbiasing factor  $c_6(n_i)$  obtained by Park and Wang (2022) and Park et al. (2022) and obtain the *unbiased* Shamos estimator given by

$$\frac{\text{Shamos}(X_i)}{c_6(n_i)}. \quad (13)$$

Thus, we can easily obtain BLUE for the Shamos case using (13) along with (12). Analogous to the case of the MAD, we have  $\text{Shamos}(X_i) = \sigma \text{Shamos}(Z_i)$ , so that we can incorporate Lemma 2 into  $\text{Shamos}(X_i)$ .

It deserves mentioning that Burr (1969) suggested the unbiased estimator of  $\sigma$ ,

$$\bar{S}_D = \frac{S_p}{c_4(N - m + 1)}, \quad (14)$$

where  $S_p^2 = \sum_{i=1}^m (n_i - 1) S_i^2 / (N - m)$ . As shown in Theorem 4 of Park and Wang (2020),  $\text{Var}(\bar{S}_C) \geq \text{Var}(\bar{S}_D)$ . Let  $\bar{\sigma}_D$  be the estimator for the scale using the MAD with analogy to  $\bar{S}_D$  above. We can consider

$$\text{MAD}(X) = \frac{\text{median}_{1 \leq i \leq m, 1 \leq j \leq n_i} |X_{ij} - \tilde{\mu}|}{\Phi^{-1}(3/4)},$$

where  $\tilde{\mu} = \text{median}_{1 \leq i \leq m, 1 \leq j \leq n_i} (X_{ij})$ . Then the unbiased estimator of  $\sigma$  is given by

$$\bar{\sigma}_D = \frac{\text{MAD}(X)}{c_5(N)}.$$

The terms related to the variance and squared unbiasing factor (possibly their ratio) under the standard normal play a role in the calculation of its variance. We observe from Figure 1 that these values change like a saw due to the nature of the different median calculations with even and odd sample sizes. Thus, as with the case of  $\bar{\sigma}_A$  and  $\bar{\sigma}_B$ , the inequality of  $\text{Var}(\bar{\sigma}_C) \geq \text{Var}(\bar{\sigma}_D)$  may not hold. Park and Wang (2020) numerically showed that the performances of  $\bar{S}_C$  and  $\bar{S}_D$  are very

close in all the performance measures although  $\bar{S}_D$  is slightly better with respect to the relative efficiency (RE), the average run length (ARL), and the standard deviation of run length (SRDL). Thus, we here consider only the three types of estimators denoted by  $A$ ,  $B$ ,  $C$  as above.

### 3 Performance of the process parameter estimators

In this section, we compare the performance of the proposed methods in (5) and (11) under no data contamination and under data contamination as well.

#### 3.1 Performance under no contamination

First, we use the RE defined as the ratio of their variances. Let  $\hat{\theta}_0$  and  $\hat{\theta}_1$  be two estimators with  $\hat{\theta}_0$  being a baseline or reference estimator. Then the RE (in percentage) of  $\hat{\theta}_1$  with respect to  $\hat{\theta}_0$  is defined as

$$\text{RE}(\hat{\theta}_1 | \hat{\theta}_0) = \frac{\text{Var}(\hat{\theta}_0)}{\text{Var}(\hat{\theta}_1)} \times 100. \quad (15)$$

We consider three samples with the four different scenarios. The sample sizes of each scenario are given by

- (a)  $n_1 = 3, n_2 = 10, n_3 = 17,$
- (b)  $n_1 = 5, n_2 = 10, n_3 = 15,$
- (c)  $n_1 = 7, n_2 = 10, n_3 = 13,$
- (d)  $n_1 = 9, n_2 = 10, n_3 = 11.$

We generate  $X_{ij}$ 's from the normal distribution with mean  $\mu_0 = 100$  and standard deviation  $\sigma_0 = 10$ . For each of the above four scenarios, we estimate  $\mu_0$  using the three types of estimation methods ( $\bar{\mu}_A, \bar{\mu}_B, \bar{\mu}_C$ ) with the mean, median, and HL estimators, respectively. Similarly, we estimate  $\sigma_0$  using the three types of estimation methods ( $\bar{\sigma}_A, \bar{\sigma}_B, \bar{\sigma}_C$ ) with the standard deviation, MAD, and Shamos estimators, respectively. We repeat each simulation one million times ( $I = 10^6$ ) to obtain the empirical variances and RE values which are provided in Table 1. We here calculate the RE values with respect to the BLUE of the mean for  $\mu_0$  and the BLUE of the standard deviation for  $\sigma_0$ . Thus, the RE of the mean with type C is always 100% and that of the standard deviation with type C is also 100%. We summarize the values of RE in Figure 2 (location estimators) and Figure 3 (scale estimators).

As seen in Figures 2 and 3, the mean and standard deviation with type C is the best as expected. For the location case, the median does not perform well, but the HL with type C is nearly as efficient

as the mean. For the scale case, the MAD performs poorly, but the Shamos with type C performs well. It should be noted that for most cases, the performance with type B is better than that with type A, but for the Shamos case with small samples, the performance with type A is better than that with type B as seen in Figure 3 (a) and (b).

### 3.2 Performance under contamination

Next, we compare the performance of the proposed methods in (5) and (11) when there is data contamination. Since the estimators tend to be biased in the presence of data contamination, we use the ratio of two mean square errors (MSEs) instead of the ratio of two variances; see, for example, Park and Leeds (2016) and Park et al. (2017, 2021). Note that using the ratio of the two MSEs allows one to compare the performance of the estimators based on their variance and bias as well. Then we have  $\text{RE}(\hat{\theta}_1 | \hat{\theta}_0) = \text{MSE}(\hat{\theta}_0)/\text{MSE}(\hat{\theta}_1) \times 100$  (in percentage). By using the estimator with no contamination data as the baseline estimator, we have

$$\text{RE}(\hat{\theta}_1 | \hat{\theta}_0) = \frac{\text{MSE}(\hat{\theta}_0) \text{ with no contamination}}{\text{MSE}(\hat{\theta}_1) \text{ with contamination}} \times 100. \quad (16)$$

We still consider three samples with the four different scenarios with the sample sizes of each scenario given by (a)  $n_1 = 3, n_2 = 10, n_3 = 17$ ; (b)  $n_1 = 5, n_2 = 10, n_3 = 15$ ; (c)  $n_1 = 7, n_2 = 10, n_3 = 13$ ; and (d)  $n_1 = 9, n_2 = 10, n_3 = 11$ . For the three samples, we generated  $X_{ij}$  from the normal distribution with mean  $\mu_0 = 100$  and standard deviation  $\sigma_0 = 10$ . It should be noted that there are estimators where a single bad observation can break down estimators. For more details, one can refer to Section 11.2 of Huber and Ronchetti (2009). To investigate the impact of a single bad observation, we contaminate only the last observation in the second sample by adding  $\delta = 100$ . Then, for each of the above four scenarios, we estimate  $\mu_0$  and  $\sigma_0$  using the three types of estimation methods as we did in Section 3. We repeat this simulation one million times ( $I = 10^6$ ) to obtain the empirical biases, variances, MSE, and RE values summarized Table 2 (scenario a), Table 3 (scenario b), Table 4 (scenario c), and Table 5 (scenario d). In addition, the MSE values (with squared empirical biases and variances) are plotted in Figure 4 for the location estimators and Figure 5 for the scale estimators. The results clearly show that the conventional estimators (sample mean and standard deviation) are very sensitive to data contamination, so that they are seriously biased (even with a single contaminated value), which can seriously degrade the performance of the conventional estimators. The RE values are summarized in Figures 6 and 7, which also show the underperformance of the conventional estimators.

Table 1: Estimated variances and relative efficiency.

|   | Location estimator |        |        |        |        | Scale estimator |         |        |
|---|--------------------|--------|--------|--------|--------|-----------------|---------|--------|
|   | mean               | median | HL1    | HL2    | HL3    | SD              | MAD     | Shamos |
| Sample sizes: $n_1 = 3, n_2 = 10, n_3 = 17$ |                    |        |        |        |        |                 |         |        |
| Variance                                    |                    |        |        |        |        |                 |         |        |
| A   | 5.4645             | 7.5319 | 5.8887 | 5.6722 | 5.8952 | 4.0281          | 10.0563 | 4.6174 |
| B   | 3.3335             | 4.8851 | 3.5346 | 3.5459 | 3.5465 | 3.7081          | 7.7644  | 5.5640 |
| C   | 3.3335             | 4.8711 | 3.5344 | 3.5452 | 3.5463 | 1.9040          | 4.8842  | 2.3609 |
| RE (%)                                      |                    |        |        |        |        |                 |         |        |
| A   | 61.00              | 44.26  | 56.61  | 58.77  | 56.55  | 47.27           | 18.93   | 41.24  |
| B   | 100.0              | 68.24  | 94.31  | 94.01  | 93.99  | 51.35           | 24.52   | 34.22  |
| C   | 100.0              | 68.44  | 94.32  | 94.03  | 94.00  | 100.0           | 38.98   | 80.65  |
| Sample sizes: $n_1 = 5, n_2 = 10, n_3 = 15$ |                    |        |        |        |        |                 |         |        |
| Variance                                    |                    |        |        |        |        |                 |         |        |
| A   | 4.0707             | 5.8565 | 4.3195 | 4.3723 | 4.3577 | 2.5087          | 6.4081  | 3.3051 |
| B   | 3.3335             | 4.8830 | 3.5306 | 3.5681 | 3.5493 | 2.4585          | 6.0195  | 3.4176 |
| C   | 3.3335             | 4.8732 | 3.5306 | 3.5681 | 3.5493 | 1.9070          | 4.8877  | 2.4273 |
| RE (%)                                      |                    |        |        |        |        |                 |         |        |
| A   | 81.89              | 56.92  | 77.17  | 76.24  | 76.49  | 76.01           | 29.76   | 57.70  |
| B   | 100.00             | 68.27  | 94.41  | 93.42  | 93.91  | 76.57           | 31.68   | 55.80  |
| C   | 100.00             | 68.40  | 94.41  | 93.42  | 93.92  | 100.00          | 39.01   | 78.56  |
| Sample sizes: $n_1 = 7, n_2 = 10, n_3 = 13$ |                    |        |        |        |        |                 |         |        |
| Variance                                    |                    |        |        |        |        |                 |         |        |
| A   | 3.5502             | 5.1726 | 3.7679 | 3.8218 | 3.7973 | 2.0747          | 5.3268  | 2.6692 |
| B   | 3.3335             | 4.8812 | 3.5334 | 3.5796 | 3.5561 | 2.0644          | 5.2467  | 2.6906 |
| C   | 3.3335             | 4.8734 | 3.5334 | 3.5795 | 3.5561 | 1.9082          | 4.8935  | 2.4319 |
| RE (%)                                      |                    |        |        |        |        |                 |         |        |
| A   | 93.90              | 64.45  | 88.47  | 87.22  | 87.79  | 91.97           | 35.82   | 71.49  |
| B   | 100.00             | 68.29  | 94.34  | 93.13  | 93.74  | 92.43           | 36.37   | 70.92  |
| C   | 100.00             | 68.40  | 94.34  | 93.13  | 93.74  | 100.00          | 38.99   | 78.46  |
| Sample sizes: $n_1 = 9, n_2 = 10, n_3 = 11$ |                    |        |        |        |        |                 |         |        |
| Variance                                    |                    |        |        |        |        |                 |         |        |
| A   | 3.3552             | 4.9101 | 3.5543 | 3.5995 | 3.5734 | 1.9249          | 4.9478  | 2.4608 |
| B   | 3.3335             | 4.8812 | 3.5318 | 3.5751 | 3.5498 | 1.9240          | 4.9419  | 2.4629 |
| C   | 3.3335             | 4.8737 | 3.5318 | 3.5751 | 3.5499 | 1.9084          | 4.8914  | 2.4403 |
| RE (%)                                      |                    |        |        |        |        |                 |         |        |
| A   | 99.35              | 67.89  | 93.79  | 92.61  | 93.29  | 99.14           | 38.57   | 77.56  |
| B   | 100.00             | 68.29  | 94.39  | 93.24  | 93.91  | 99.18           | 38.62   | 77.49  |
| C   | 100.00             | 68.40  | 94.39  | 93.24  | 93.91  | 100.00          | 39.01   | 78.20  |

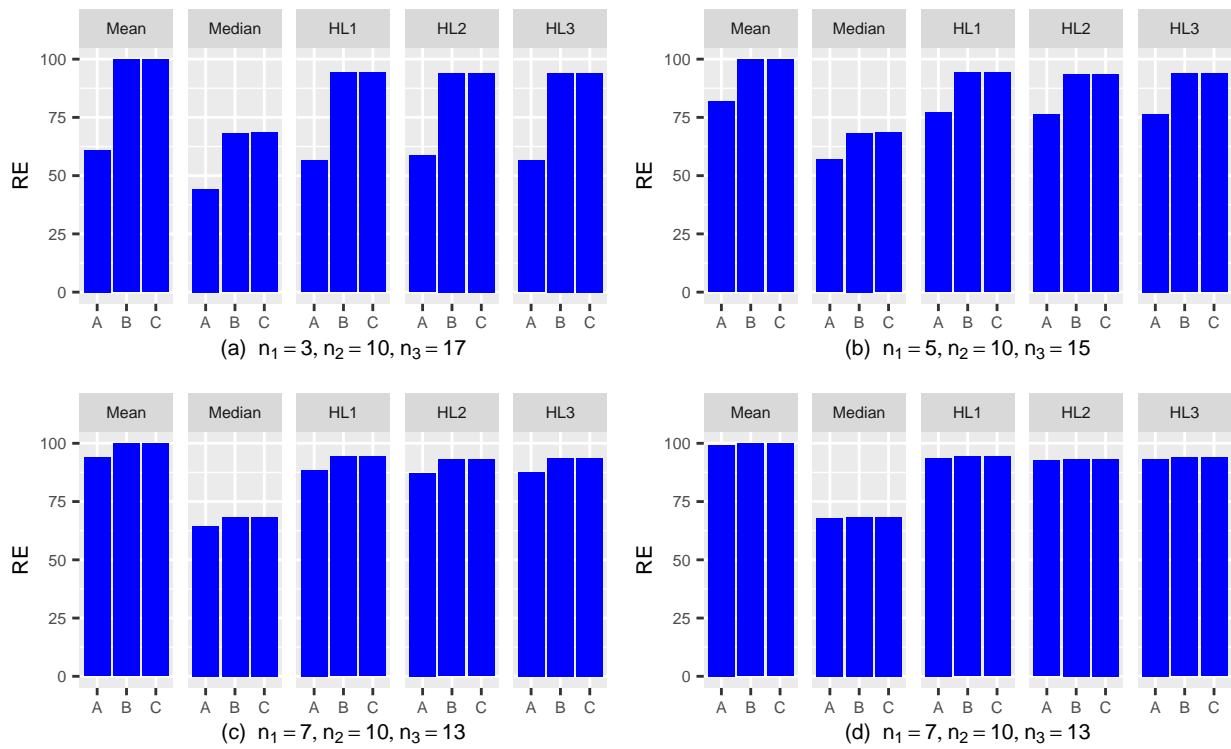


Figure 2: Relative efficiency of the location estimators under consideration with different sample sizes.

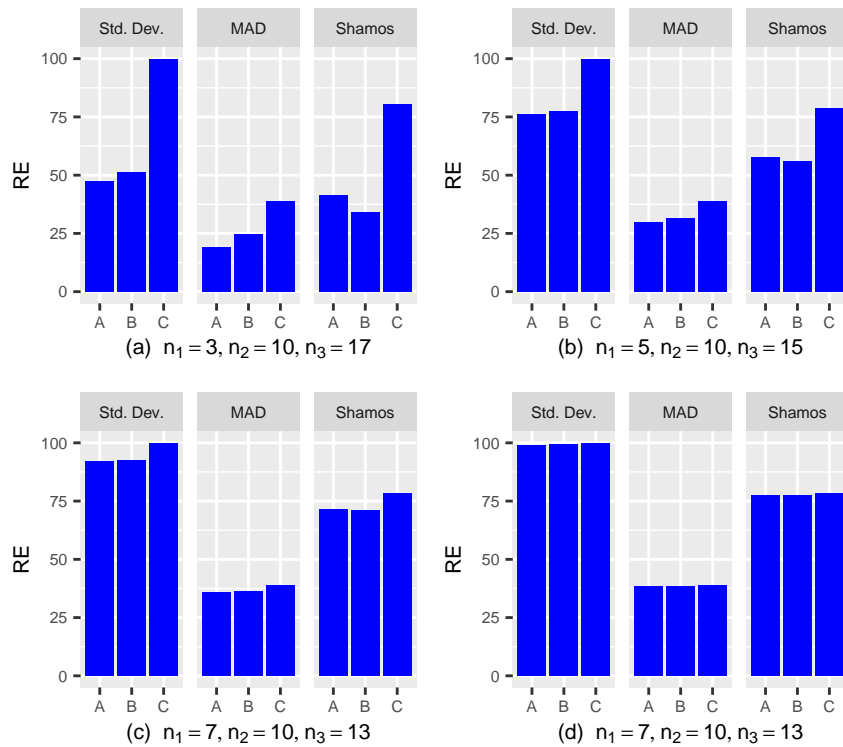


Figure 3: Relative efficiency of the scale estimators under consideration with different sample sizes.

Table 2: Estimated variances and biases ( $n_1 = 3$ ,  $n_2 = 10$ ,  $n_3 = 17$ ).

|          | Location estimator |        |        |        |        | Scale estimator |         |        |
|----------|--------------------|--------|--------|--------|--------|-----------------|---------|--------|
|          | mean               | median | HL1    | HL2    | HL3    | SD              | MAD     | Shamos |
| Variance |                    |        |        |        |        |                 |         |        |
| A        | 5.4645             | 7.6923 | 6.0507 | 5.8341 | 6.0557 | 4.6532          | 10.4937 | 5.2532 |
| B        | 3.3335             | 5.0457 | 3.6957 | 3.7070 | 3.7050 | 4.3662          | 8.2691  | 6.1166 |
| C        | 3.3335             | 5.0494 | 3.6951 | 3.7029 | 3.7056 | 2.5255          | 5.3738  | 2.9547 |
| Bias     |                    |        |        |        |        |                 |         |        |
| A        | 3.3331             | 0.4574 | 0.6964 | 0.6593 | 0.6776 | 7.9802          | 0.5116  | 1.0234 |
| B        | 3.3337             | 0.4580 | 0.6970 | 0.6598 | 0.6782 | 8.1896          | 0.5515  | 0.9536 |
| C        | 3.3337             | 0.4831 | 0.6962 | 0.6526 | 0.6777 | 7.9654          | 0.5475  | 0.9904 |
| MSE      |                    |        |        |        |        |                 |         |        |
| A        | 16.5743            | 7.9016 | 6.5357 | 6.2688 | 6.5148 | 68.3374         | 10.7554 | 6.3005 |
| B        | 14.4472            | 5.2555 | 4.1815 | 4.1424 | 4.1659 | 71.4353         | 8.5733  | 7.0258 |
| C        | 14.4472            | 5.2827 | 4.1798 | 4.1289 | 4.1648 | 65.9724         | 5.6735  | 3.9356 |
| RE (%)   |                    |        |        |        |        |                 |         |        |
| A        | 20.11              | 42.19  | 51.00  | 53.18  | 51.17  | 2.79            | 17.70   | 30.22  |
| B        | 23.07              | 63.43  | 79.72  | 80.47  | 80.02  | 2.67            | 22.21   | 27.10  |
| C        | 23.07              | 63.10  | 79.75  | 80.74  | 80.04  | 2.89            | 33.56   | 48.38  |

Table 3: Estimated variances and biases ( $n_1 = 5$ ,  $n_2 = 10$ ,  $n_3 = 15$ ).

|          | Location estimator |        |        |        |        | Scale estimator |        |        |
|----------|--------------------|--------|--------|--------|--------|-----------------|--------|--------|
|          | mean               | median | HL1    | HL2    | HL3    | SD              | MAD    | Shamos |
| Variance |                    |        |        |        |        |                 |        |        |
| A        | 4.0707             | 6.0165 | 4.4794 | 4.5301 | 4.5147 | 3.1293          | 6.8324 | 3.9380 |
| B        | 3.3335             | 5.0432 | 3.6917 | 3.7270 | 3.7076 | 3.0890          | 6.4620 | 4.0363 |
| C        | 3.3335             | 5.0515 | 3.6911 | 3.7256 | 3.7076 | 2.5256          | 5.3755 | 3.0535 |
| Bias     |                    |        |        |        |        |                 |        |        |
| A        | 3.3331             | 0.4599 | 0.6983 | 0.6613 | 0.6798 | 7.9751          | 0.5136 | 1.0226 |
| B        | 3.3337             | 0.4603 | 0.6989 | 0.6617 | 0.6802 | 8.0385          | 0.5243 | 1.0110 |
| C        | 3.3337             | 0.4857 | 0.6975 | 0.6588 | 0.6802 | 7.9705          | 0.5499 | 1.0170 |
| MSE      |                    |        |        |        |        |                 |        |        |
| A        | 15.1801            | 6.2280 | 4.9669 | 4.9674 | 4.9769 | 66.7314         | 7.0963 | 4.9836 |
| B        | 14.4472            | 5.2551 | 4.1802 | 4.1648 | 4.1703 | 67.7067         | 6.7369 | 5.0584 |
| C        | 14.4472            | 5.2874 | 4.1775 | 4.1595 | 4.1702 | 66.0547         | 5.6779 | 4.0877 |
| RE (%)   |                    |        |        |        |        |                 |        |        |
| A        | 21.96              | 53.52  | 67.11  | 67.11  | 66.98  | 2.86            | 26.87  | 38.27  |
| B        | 23.07              | 63.43  | 79.74  | 80.04  | 79.93  | 2.82            | 28.31  | 37.70  |
| C        | 23.07              | 63.05  | 79.80  | 80.14  | 79.94  | 2.89            | 33.59  | 46.65  |

Table 4: Estimated variances and biases ( $n_1 = 7$ ,  $n_2 = 10$ ,  $n_3 = 13$ ).

|          | Location estimator |        |        |        |        | Scale estimator |        |        |
|----------|--------------------|--------|--------|--------|--------|-----------------|--------|--------|
|          | mean               | median | HL1    | HL2    | HL3    | SD              | MAD    | Shamos |
| Variance |                    |        |        |        |        |                 |        |        |
| A        | 3.5502             | 5.3307 | 3.9263 | 3.9794 | 3.9536 | 2.6910          | 5.7545 | 3.3054 |
| B        | 3.3335             | 5.0403 | 3.6926 | 3.7380 | 3.7133 | 2.6835          | 5.6769 | 3.3238 |
| C        | 3.3335             | 5.0507 | 3.6922 | 3.7377 | 3.7139 | 2.5240          | 5.3844 | 3.0612 |
| Bias     |                    |        |        |        |        |                 |        |        |
| A        | 3.3341             | 0.4592 | 0.6969 | 0.6598 | 0.6779 | 7.9805          | 0.5090 | 1.0211 |
| B        | 3.3337             | 0.4587 | 0.6965 | 0.6594 | 0.6776 | 7.9985          | 0.5106 | 1.0186 |
| C        | 3.3337             | 0.4843 | 0.6957 | 0.6589 | 0.6789 | 7.9796          | 0.5466 | 1.0165 |
| MSE      |                    |        |        |        |        |                 |        |        |
| A        | 14.6663            | 5.5415 | 4.4120 | 4.4148 | 4.4131 | 66.3798         | 6.0137 | 4.3480 |
| B        | 14.4472            | 5.2507 | 4.1778 | 4.1728 | 4.1724 | 66.6592         | 5.9377 | 4.3613 |
| C        | 14.4472            | 5.2853 | 4.1762 | 4.1718 | 4.1748 | 66.1982         | 5.6832 | 4.0943 |
| RE (%)   |                    |        |        |        |        |                 |        |        |
| A        | 22.73              | 60.16  | 75.56  | 75.51  | 75.54  | 2.87            | 31.73  | 43.89  |
| B        | 23.07              | 63.49  | 79.79  | 79.89  | 79.90  | 2.86            | 32.14  | 43.75  |
| C        | 23.07              | 63.07  | 79.82  | 79.91  | 79.85  | 2.88            | 33.58  | 46.60  |

Table 5: Estimated variances and biases ( $n_1 = 9$ ,  $n_2 = 10$ ,  $n_3 = 11$ ).

|          | Location estimator |        |        |        |        | Scale estimator |        |        |
|----------|--------------------|--------|--------|--------|--------|-----------------|--------|--------|
|          | mean               | median | HL1    | HL2    | HL3    | SD              | MAD    | Shamos |
| Variance |                    |        |        |        |        |                 |        |        |
| A        | 3.3552             | 5.0699 | 3.7179 | 3.7616 | 3.7344 | 2.5416          | 5.3737 | 3.0974 |
| B        | 3.3335             | 5.0408 | 3.6955 | 3.7373 | 3.7110 | 2.5410          | 5.3650 | 3.0989 |
| C        | 3.3335             | 5.0519 | 3.6952 | 3.7368 | 3.7114 | 2.5248          | 5.3815 | 3.0763 |
| Bias     |                    |        |        |        |        |                 |        |        |
| A        | 3.3338             | 0.4602 | 0.6979 | 0.6609 | 0.6791 | 7.9790          | 0.5122 | 1.0233 |
| B        | 3.3337             | 0.4602 | 0.6978 | 0.6608 | 0.6790 | 7.9808          | 0.5106 | 1.0227 |
| C        | 3.3337             | 0.4858 | 0.6972 | 0.6599 | 0.6799 | 7.9790          | 0.5495 | 1.0230 |
| MSE      |                    |        |        |        |        |                 |        |        |
| A        | 14.4696            | 5.2817 | 4.2050 | 4.1984 | 4.1957 | 66.2064         | 5.6360 | 4.1446 |
| B        | 14.4472            | 5.2526 | 4.1824 | 4.1739 | 4.1720 | 66.2346         | 5.6257 | 4.1448 |
| C        | 14.4472            | 5.2879 | 4.1814 | 4.1723 | 4.1736 | 66.1897         | 5.6834 | 4.1229 |
| RE (%)   |                    |        |        |        |        |                 |        |        |
| A        | 23.04              | 63.11  | 79.27  | 79.40  | 79.45  | 2.88            | 33.86  | 46.04  |
| B        | 23.07              | 63.46  | 79.70  | 79.87  | 79.90  | 2.88            | 33.92  | 46.04  |
| C        | 23.07              | 63.04  | 79.72  | 79.90  | 79.87  | 2.88            | 33.58  | 46.29  |

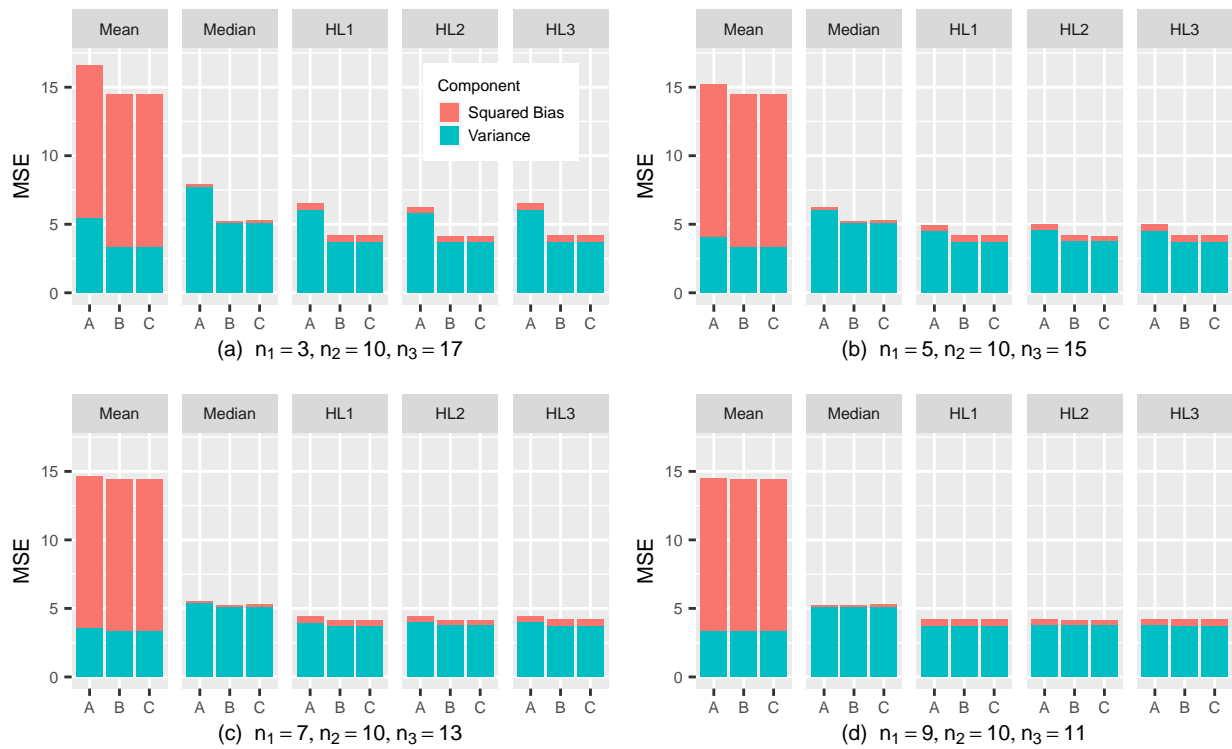


Figure 4: MSE of the location estimators under consideration with different sample sizes.

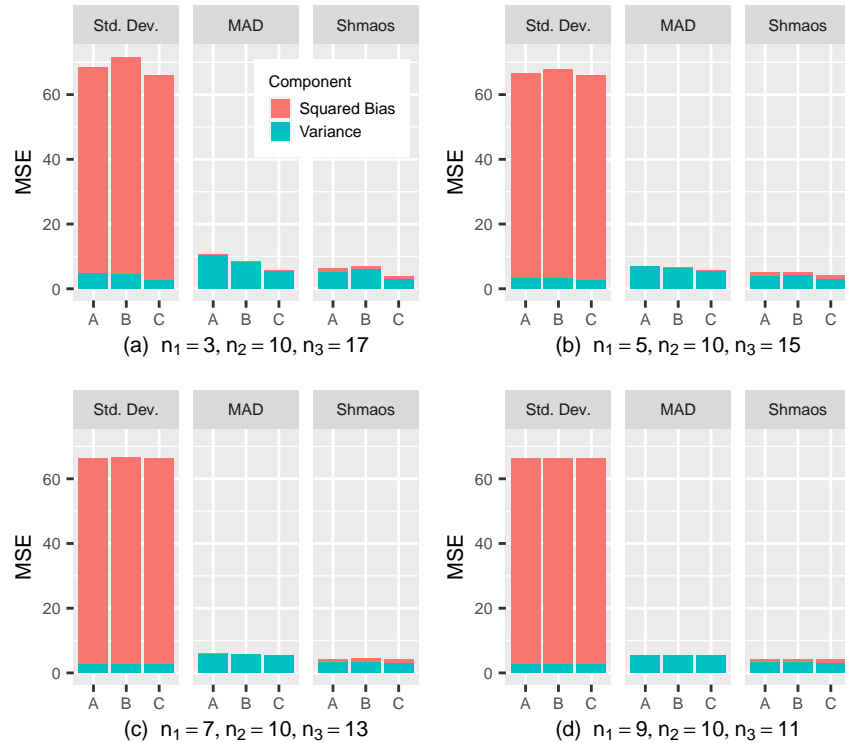


Figure 5: MSE of the scale estimators under consideration with different sample sizes.



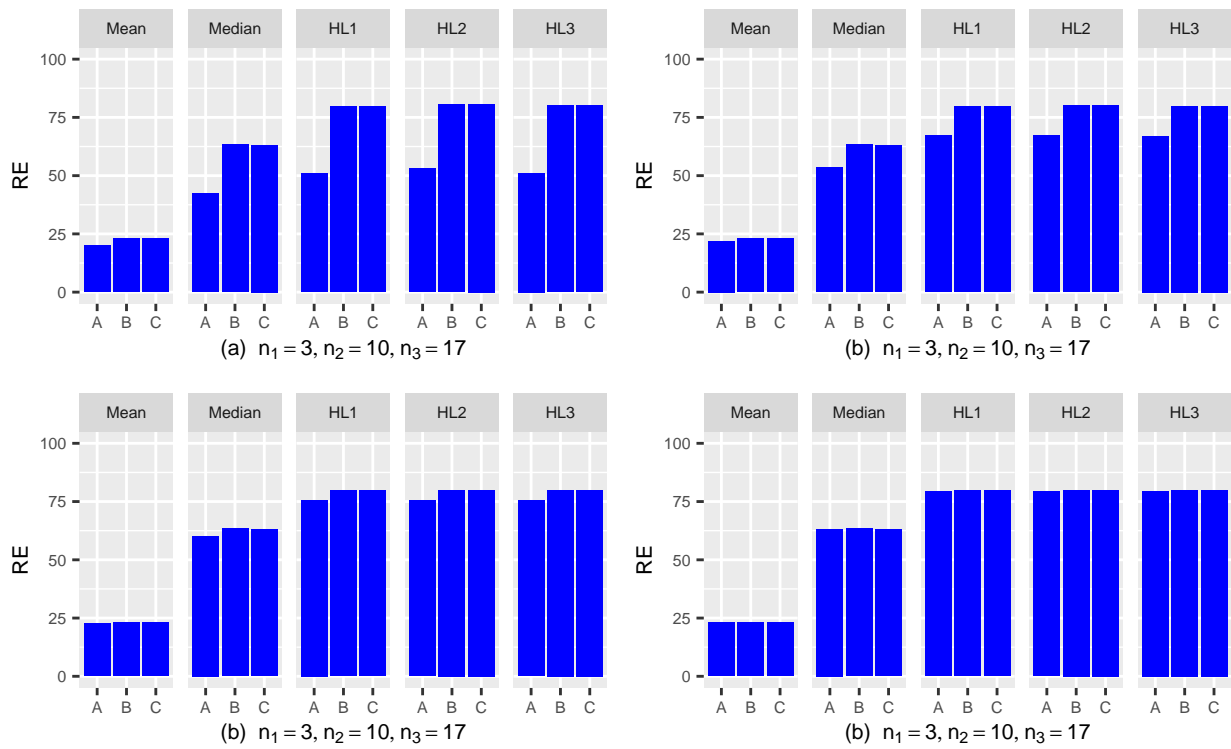


Figure 6: Relative efficiency of the location estimators under consideration with different sample sizes.

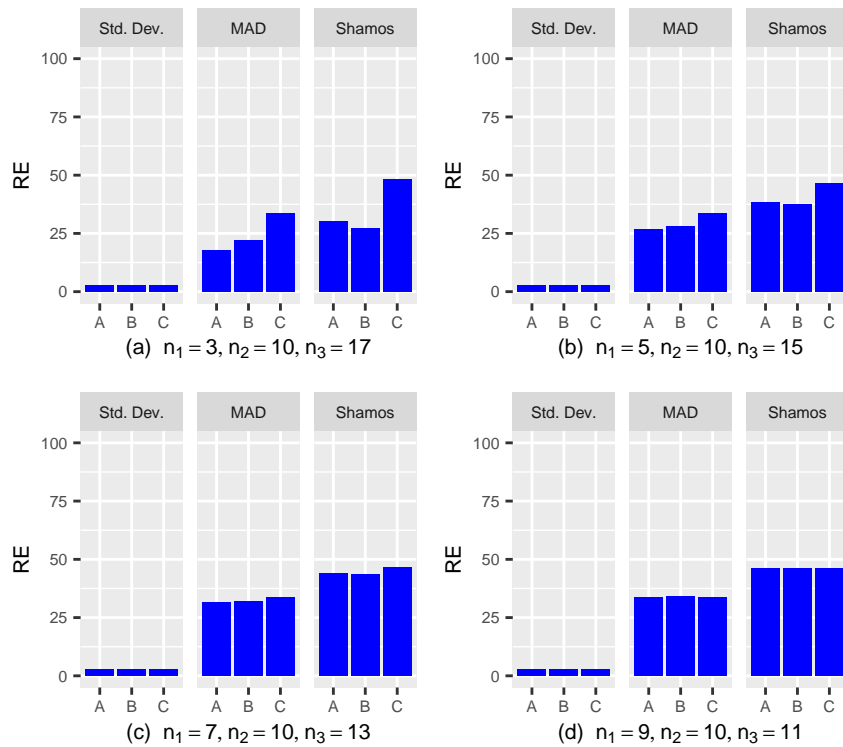


Figure 7: Relative efficiency of the scale estimators under consideration with different sample sizes.

## 4 Construction of robust $\bar{X}$ control chart with unequal sample sizes

We briefly introduce how to construct the control charts and then discuss how to implement the proposed estimators in (5) and (11) to construct the robust  $\bar{X}$  charts with unequal sample sizes. We assume that we have  $m$  samples from Phase-I period and that each sample in Phase-I has different sample sizes, denoted by  $n_i$  where  $i = 1, 2, \dots, m$ . Then, we monitor the process with a sample of size  $n_k$  in Phase-II.

### 4.1 Construction of robust $\bar{X}$ chart

It is well-known that the statistical asymptotic theory has

$$\frac{\bar{X}_k - E(\bar{X}_k)}{\text{SE}(\bar{X}_k)} \xrightarrow{d} N(0, 1),$$

where  $\xrightarrow{d}$  denotes the convergence in distribution and  $\bar{X}_k$  is the sample mean with sample size  $n_k$ . Solving  $(\bar{X}_k - E(\bar{X}_k))/\text{SE}(\bar{X}_k) = \pm g$  for  $\bar{X}_k$ , we have the CL  $\pm g \cdot \text{SE}$  control limits given by

$$E(\bar{X}_k) \pm g \cdot \text{SE}(\bar{X}_k) = \mu \pm g \cdot \frac{\sigma}{\sqrt{n_k}}.$$

The population parameters,  $\mu$  and  $\sigma$ , are generally unknown and need to be estimated in Phase-I period. As long as we obtain the estimates,  $\hat{\mu}$  and  $\hat{\sigma}$ , we have UCL =  $\hat{\mu} + g\hat{\sigma}/\sqrt{n_k}$ , CL =  $\hat{\mu}$ , and LCL =  $\hat{\mu} - g\hat{\sigma}/\sqrt{n_k}$ .

To estimate  $\mu$ , one can use any type of  $\tilde{\mu}_A$  in (3),  $\tilde{\mu}_B$  in (2), and  $\tilde{\mu}_C$  in (5). For  $\sigma$ , one can use any type of  $\tilde{\sigma}_A$  in (8),  $\tilde{\sigma}_B$  in (9), and  $\tilde{\sigma}_C$  in (11). As an illustration, using  $\tilde{\mu}_A$  and  $\tilde{\sigma}_A$  with the American Standard, we have  $\bar{X}$  chart as follows:

$$\begin{aligned} \text{UCL}_A &= \tilde{\mu}_A + \frac{3\tilde{\sigma}_A}{\sqrt{n_k}} \\ \text{CL}_A &= \tilde{\mu}_A \\ \text{LCL}_A &= \tilde{\mu}_A - \frac{3\tilde{\sigma}_A}{\sqrt{n_k}}. \end{aligned}$$

We consider the following combinations for each of the three different estimation methods.

Method-I: using the sample mean and standard deviation.

Method-II: using the median and MAD.

Method-III: using the HL and Shamos.

Note that the combination of the sample mean and standard deviation performs the best under no contamination although they have a zero breakdown point. Also, the combination of the median

and MAD was chosen because both estimators have a breakdown point of 50%. Both the HL and Shamos estimators have a breakdown point of 29% and perform well in both the presence and absence of contamination.

## 4.2 Numerical studies

We carry out extensive Monte Carlo simulations to compare the performance of the proposed  $\bar{X}$  charts with respect to the ARL, SDRL and the percentile of run length (PRL) of the run lengths (RLs). In Phase-I, we consider the following five different plans. Each plan has fifteen samples and their sample sizes are given as follow.

Plan-1:  $n_1 = n_2 = \dots = n_5 = 3$ ,  $n_6 = n_7 = \dots = n_{10} = 10$ ,  $n_{11} = n_{12} = \dots = n_{15} = 17$

Plan-2:  $n_1 = n_2 = \dots = n_5 = 5$ ,  $n_6 = n_7 = \dots = n_{10} = 10$ ,  $n_{11} = n_{12} = \dots = n_{15} = 15$

Plan-3:  $n_1 = n_2 = \dots = n_5 = 7$ ,  $n_6 = n_7 = \dots = n_{10} = 10$ ,  $n_{11} = n_{12} = \dots = n_{15} = 13$

Plan-4:  $n_1 = n_2 = \dots = n_5 = 9$ ,  $n_6 = n_7 = \dots = n_{10} = 10$ ,  $n_{11} = n_{12} = \dots = n_{15} = 11$

Plan-5:  $n_1 = n_2 = \dots = n_5 = 10$ ,  $n_6 = n_7 = \dots = n_{10} = 10$ ,  $n_{11} = n_{12} = \dots = n_{15} = 10$

We generate  $X_{ij}$  from the normal distribution with  $\mu_0 = 100$  and  $\sigma_0 = 5$  in Phase-I. Then we construct control charts using each of the three types:  $(\bar{\hat{\mu}}_A, \bar{\hat{\sigma}}_A)$  pair,  $(\bar{\hat{\mu}}_B, \bar{\hat{\sigma}}_B)$  pair, and  $(\bar{\hat{\mu}}_C, \bar{\hat{\sigma}}_C)$  pair with each of the three different estimation methods. Then, in Phase-II, we monitor the process with a sample of size  $n_k = 10$  from the same normal distribution. By repeating this experiment  $I = 100,000$  times, we obtain the 100,000 run lengths and calculate the ARL, SDRL, PRL, and skewness of RLs, which are reported in Table 6. We also draw the box-percentile plots with all 99 percentiles shown in Figure 8. For brevity, we considered only Plan-1, Plan-3 and Plan-5 for the box-percentile plots. Considering that the desired  $ARL_0$  is 370, the pooling type C clearly outperforms for all the methods under consideration. We can also observe that Method-I and Method-III are quite comparable, while Method-II underperforms. Also, this can be observed from Figure 8.

To investigate the effect of data contamination, we add a value ( $\delta = 100$ ) in the last observation of the fifteenth sample for all five plans in Phase-I. Again, we repeat this experiment  $I = 100,000$  times and calculate the ARL, SDRL, PRL, and skewness, which are provided in Table 7 and Figure 9. Numerical results clearly show that the values using Method I change dramatically, while those using Method II and Method III are almost kept unchanged. This observation clearly shows the superiority of the proposed chart based on the process estimators in (5) and (11).

Table 6: Estimated ARL, SDRL, PRL (99%), and skewness of the RLs for the  $\bar{X}$  charts based on three different methods ( $n_k = 10$ ) with no contamination.

|          | Method-I   |        |        | Method-II |         |        | Method-III |        |        |
|----------|--|--------|--------|-----------|---------|--------|------------|--------|--------|
|          | A  | B      | C      | A         | B       | C      | A          | B      | C      |
| Plan-1   | $(n_1 = n_2 = \dots = n_5 = 3, n_6 = n_7 = \dots = n_{10} = 10, n_{11} = n_{12} = \dots = n_{15} = 17)$  |        |        |           |         |        |            |        |        |
| ARL      | 476.1  | 456.5  | 366.8  | 1455.2    | 809.0   | 491.4  | 519.0      | 599.7  | 382.3  |
| SDRL     | 1196.7   | 1056.1 | 554.5  | 33077.2   | 5878.8  | 1342.5 | 1506.1     | 2253.9 | 631.0  |
| 99%      | 4457.1   | 4064.0 | 2539.0 | 17424.1   | 10264.1 | 4998.0 | 5199.0     | 6537.1 | 2819.0 |
| skewness | 25.9   | 26.4   | 6.5    | 160.4     | 72.6    | 17.9   | 25.1       | 41.7   | 7.5    |
| Plan-2   | $(n_1 = n_2 = \dots = n_5 = 5, n_6 = n_7 = \dots = n_{10} = 10, n_{11} = n_{12} = \dots = n_{15} = 15)$  |        |        |           |         |        |            |        |        |
| ARL      | 392.9  | 391.0  | 367.1  | 608.8     | 575.9   | 486.8  | 427.8      | 434.6  | 384.6  |
| SDRL     | 650.5  | 641.1  | 547.4  | 2548.2    | 2311.0  | 1351.4 | 926.8      | 957.7  | 639.0  |
| 99%      | 2977.0   | 2946.0 | 2517.0 | 6964.0    | 6387.0  | 4964.0 | 3581.0     | 3700.0 | 2885.0 |
| skewness | 7.1  | 6.9    | 6.1    | 42.1      | 46.4    | 27.7   | 26.7       | 25.1   | 7.8    |
| Plan-3   | $(n_1 = n_2 = \dots = n_5 = 7, n_6 = n_7 = \dots = n_{10} = 10, n_{11} = n_{12} = \dots = n_{15} = 13)$  |        |        |           |         |        |            |        |        |
| ARL      | 373.9  | 374.4  | 367.8  | 522.0     | 514.3   | 490.2  | 396.2      | 397.4  | 383.7  |
| SDRL     | 589.7  | 589.5  | 557.1  | 1606.7    | 1568.5  | 1482.1 | 685.2      | 690.7  | 631.3  |
| 99%      | 2676.0   | 2671.0 | 2577.0 | 5583.0    | 5419.0  | 4904.0 | 3094.0     | 3112.0 | 2865.0 |
| skewness | 7.5  | 7.5    | 7.1    | 28.3      | 29.5    | 35.6   | 7.9        | 8.0    | 7.2    |
| Plan-4   | $(n_1 = n_2 = \dots = n_5 = 9, n_6 = n_7 = \dots = n_{10} = 10, n_{11} = n_{12} = \dots = n_{15} = 11)$  |        |        |           |         |        |            |        |        |
| ARL      | 368.5  | 368.5  | 367.4  | 491.9     | 491.5   | 490.3  | 384.3      | 384.3  | 383.7  |
| SDRL     | 556.2  | 556.2  | 553.7  | 1289.7    | 1288.5  | 1333.2 | 631.0      | 631.3  | 626.5  |
| 99%      | 2549.0   | 2549.0 | 2534.0 | 5202.1    | 5177.0  | 5122.0 | 2881.0     | 2881.0 | 2866.0 |
| skewness | 6.4  | 6.4    | 6.5    | 14.7      | 14.7    | 18.4   | 6.7        | 6.7    | 6.6    |
| Plan-5   | $(n_1 = n_2 = \dots = n_5 = 10, n_6 = n_7 = \dots = n_{10} = 10, n_{11} = n_{12} = \dots = n_{15} = 10)$ |        |        |           |         |        |            |        |        |
| ARL      | 368.7  | 368.7  | 368.7  | 481.1     | 481.1   | 481.1  | 385.9      | 385.9  | 385.9  |
| SDRL     | 556.1  | 556.1  | 556.1  | 1280.2    | 1280.2  | 1280.2 | 642.2      | 642.2  | 642.2  |
| 99%      | 2545.0   | 2545.0 | 2545.0 | 4826.0    | 4826.0  | 4826.0 | 2913.0     | 2913.0 | 2913.0 |
| skewness | 6.4  | 6.4    | 6.4    | 21.1      | 21.1    | 21.1   | 7.8        | 7.8    | 7.8    |

Table 7: Estimated ARL, SDRL, PRL (99%), and skewness of the RLS for the  $\bar{X}$  charts based on three different methods ( $n_k = 10$ ) with contamination. The last value in the fifteenth sample is contaminated by adding  $\delta = 100$ .

|          | Method-I   |          |          | Method-II |         |        | Method-III |        |        |
|----------|--|----------|----------|-----------|---------|--------|------------|--------|--------|
|          | A  | B        | C        | A         | B       | C      | A          | B      | C      |
| Plan-1   | $(n_1 = n_2 = \dots = n_5 = 3, n_6 = n_7 = \dots = n_{10} = 10, n_{11} = n_{12} = \dots = n_{15} = 17)$  |          |          |           |         |        |            |        |        |
| ARL      | 6178.6   | 6587.0   | 66089.1  | 1398.6    | 850.2   | 540.2  | 579.3      | 657.6  | 466.7  |
| SDRL     | 24535.1  | 24566.0  | 175775.1 | 18574.6   | 5890.5  | 1559.6 | 1713.6     | 2447.5 | 798.0  |
| 99%      | 72414.1  | 74755.1  | 700892.6 | 18548.2   | 11143.3 | 5578.0 | 5960.1     | 7396.1 | 3569.0 |
| skewness | 35.2   | 34.6     | 18.2     | 100.2     | 95.2    | 24.0   | 22.3       | 41.8   | 7.9    |
| Plan-2   | $(n_1 = n_2 = \dots = n_5 = 5, n_6 = n_7 = \dots = n_{10} = 10, n_{11} = n_{12} = \dots = n_{15} = 15)$  |          |          |           |         |        |            |        |        |
| ARL      | 6036.8   | 6395.5   | 46438.2  | 650.3     | 613.6   | 540.8  | 486.5      | 492.1  | 470.4  |
| SDRL     | 14884.3  | 15719.9  | 121929.7 | 2682.5    | 2316.1  | 1524.5 | 1012.9     | 1042.0 | 802.5  |
| 99%      | 60810.1  | 63944.0  | 491134.8 | 7492.1    | 7027.1  | 5557.0 | 4224.1     | 4334.0 | 3596.0 |
| skewness | 14.5   | 14.3     | 16.7     | 40.2      | 41.9    | 21.9   | 12.2       | 12.0   | 7.5    |
| Plan-3   | $(n_1 = n_2 = \dots = n_5 = 7, n_6 = n_7 = \dots = n_{10} = 10, n_{11} = n_{12} = \dots = n_{15} = 13)$  |          |          |           |         |        |            |        |        |
| ARL      | 7864.9   | 8146.6   | 31086.0  | 568.1     | 561.1   | 544.0  | 458.9      | 459.7  | 474.2  |
| SDRL     | 17590.3  | 18306.0  | 79459.0  | 1768.6    | 1709.7  | 1570.0 | 825.8      | 834.9  | 821.4  |
| 99%      | 75670.8  | 79065.0  | 321388.3 | 6213.0    | 5997.0  | 5640.0 | 3663.0     | 3678.0 | 3687.0 |
| skewness | 9.5  | 9.6      | 13.8     | 22.0      | 22.0    | 20.9   | 8.3        | 8.6    | 7.6    |
| Plan-4   | $(n_1 = n_2 = \dots = n_5 = 9, n_6 = n_7 = \dots = n_{10} = 10, n_{11} = n_{12} = \dots = n_{15} = 11)$  |          |          |           |         |        |            |        |        |
| ARL      | 11724.3  | 11892.9  | 19452.7  | 545.5     | 546.2   | 546.5  | 463.7      | 463.2  | 473.9  |
| SDRL     | 25690.7  | 26153.4  | 44571.0  | 1656.1    | 1655.0  | 1597.2 | 788.9      | 788.1  | 813.3  |
| 99%      | 115429.0   | 118007.4 | 192744.8 | 5592.0    | 5618.1  | 5639.1 | 3585.0     | 3579.0 | 3679.1 |
| skewness | 8.8  | 8.7      | 10.1     | 33.1      | 33.1    | 31.0   | 7.2        | 7.2    | 7.4    |
| Plan-5   | $(n_1 = n_2 = \dots = n_5 = 10, n_6 = n_7 = \dots = n_{10} = 10, n_{11} = n_{12} = \dots = n_{15} = 10)$ |          |          |           |         |        |            |        |        |
| ARL      | 15165.5  | 15165.5  | 15165.5  | 528.5     | 528.5   | 528.5  | 473.9      | 473.9  | 473.9  |
| SDRL     | 33868.8  | 33868.8  | 33868.8  | 1323.0    | 1323.0  | 1323.0 | 800.0      | 800.0  | 800.0  |
| 99%      | 149699.4   | 149699.4 | 149699.4 | 5297.0    | 5297.0  | 5297.0 | 3676.0     | 3676.0 | 3676.0 |
| skewness | 8.7  | 8.7      | 8.7      | 13.0      | 13.0    | 13.0   | 7.0        | 7.0    | 7.0    |

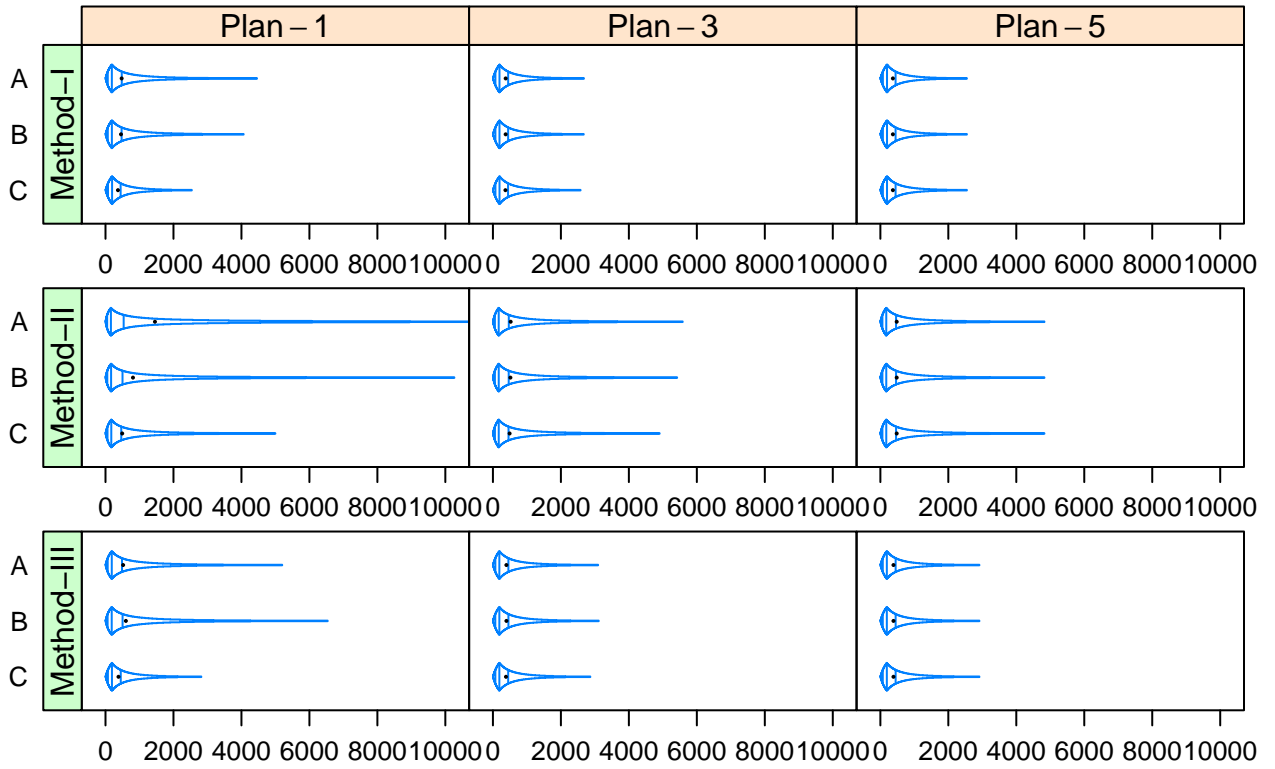


Figure 8: The box-percentile plots of the run lengths of  $\bar{X}$  charts under consideration (with no contamination).

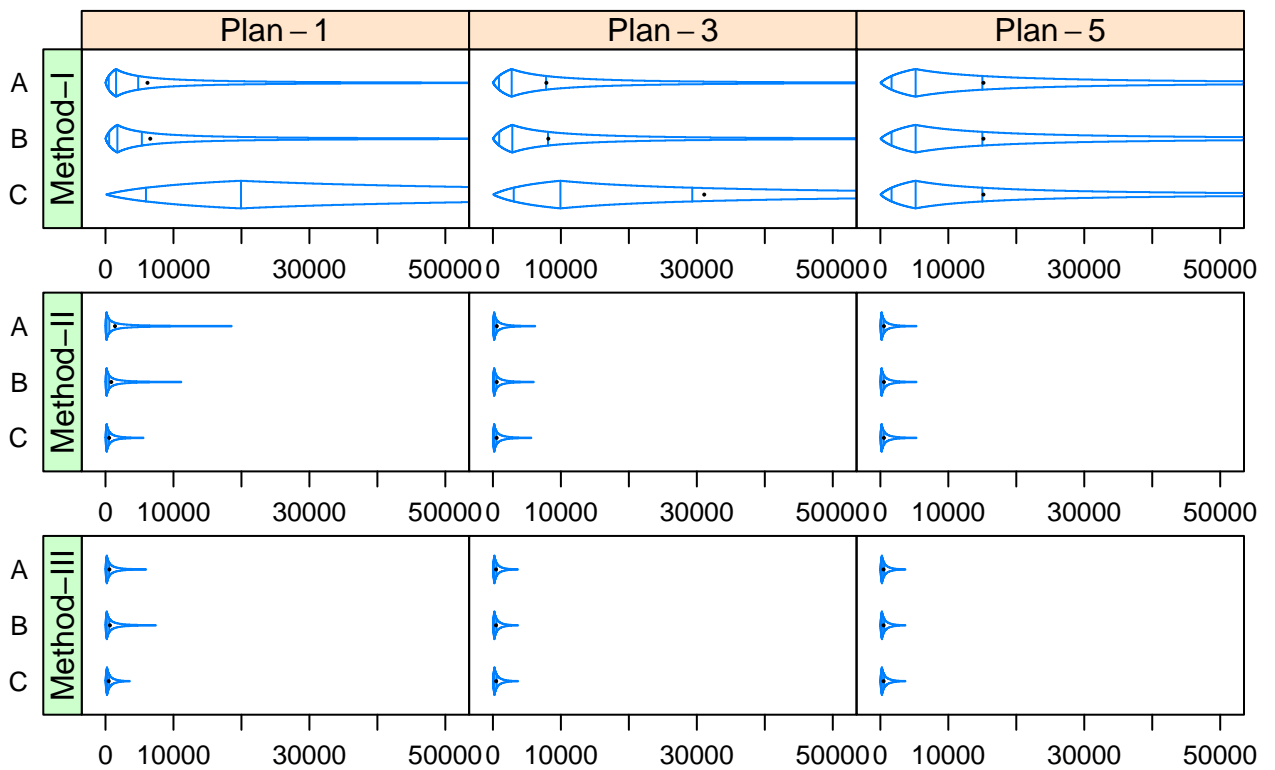


Figure 9: The box-percentile plots of the run lengths of  $\bar{X}$  charts under consideration (with contamination).

## 5 An illustrative example

In this section, we consider a real-data set from Table 6.4 of Montgomery (2013). The data set includes 113 measurements (in millimeters) of the diameters of piston rings for an automotive engine produced by a forging process. The observations were obtained from twenty-five samples and the sample sizes are given by 5, 3, 5, 5, 5, 4, 4, 5, 4, 5, 5, 5, 3, 5, 3, 5, 4, 5, 5, 3, 5, 5, 5, 5, 5. To construct the  $\bar{X}$  chart with the size  $n_k = 5$ , we used the pooling type C in (5) and (11) for all the methods (Methods-I, II, III mentioned in Subsection 4.1). It should be noted that as an estimate of  $\sigma$ , Montgomery (2013) used the square root of the pooled sample variance, which is different from the pooled standard deviation with the pooling type C.

Table 8: Control limits of the  $\bar{X}$  charts with  $n_k = 5$ .

|            |          |          |          |
|------------|----------|----------|----------|
| Montgomery | 73.98606 | 74.00075 | 74.01544 |
| Method-I   | 73.98693 | 74.00075 | 74.01457 |
| Method-II  | 73.98650 | 74.00139 | 74.01629 |
| Method-III | 73.98644 | 74.00072 | 74.01499 |

In this example, we investigate the sensitivity of the considered methods due to data contamination. To be more specific, we add a single contaminated observation (denoted by  $\delta$ ) in the first sample and then calculate LCL, CL, and UCL. To further investigate their effect due to the level of contaminated value, we changed the value of  $\delta$  in a grid-like fashion such as  $\delta = 73(0.1)74$ . Then we consider an empirical approach analogous to the underlying spirit of the influence function by investigating how any method is affected by the level of contaminated value. For the illustrative examples on the implementation of this empirical procedure, one may refer to Figure 5 of Park and Basu (2011) and Figure 3 of Park et al. (2022). Numerical results are depicted in Figure 10. We observe that the  $\bar{X}$  control charts based on Montgomery (2013) and Method-I are very sensitive to contamination, whereas those based on Method-II and Method-III are quite robust.

## 6 Concluding remarks

In this paper, we have developed robust  $\bar{X}$  charts, which can simultaneously deal with the issues of unequal sample sizes and data contamination. We showed that in the construction of an  $\bar{X}$  control chart with unequal sample sizes, special care should be taken, because inappropriate pooling of estimates from different sample sizes can lead to misleading results. To overcome this challenge, we have proposed the two process parameter estimation methods in (5) (location) and (11) (scale)

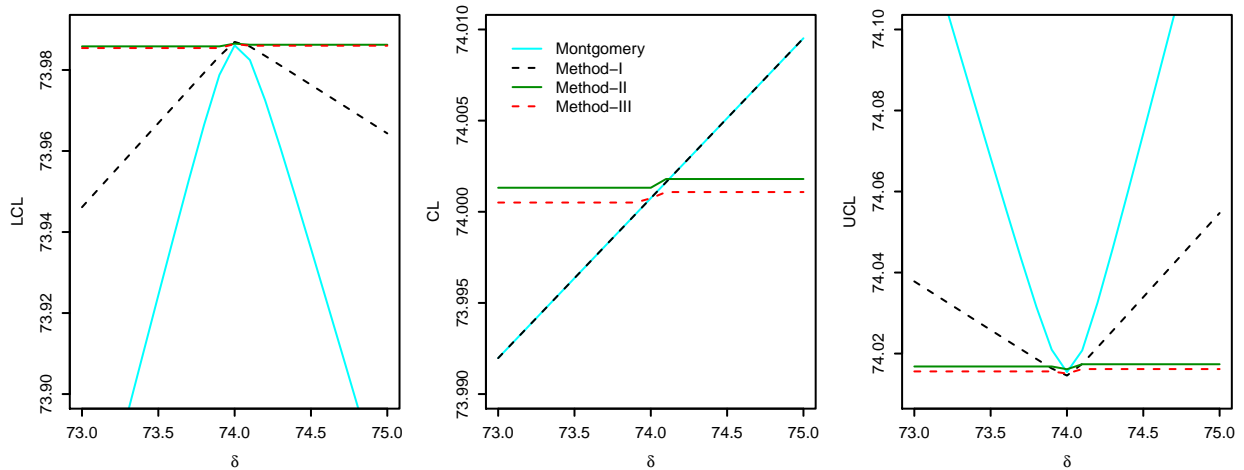


Figure 10: LCL, CL and UCL of  $\bar{X}$  chart, and their effect due to the amount of contamination level ( $\delta$ ).

for optimal pooling in the sense that they are the BLUEs for the unknown process parameters. In addition, we have investigated the effect of data contamination on the performance of robust  $\bar{X}$  charts with these BLUEs in terms of the ARL, SDRL, PRL and skewness. Numerical results from extensive Monte Carlo simulations and a real data analysis revealed that the traditional variable control charts seriously underperform for monitoring process in the presence of data contamination and are extremely sensitive to even a single contaminated value, while the proposed robust  $\bar{X}$  control charts outperform in a manner that is comparable with existing ones, whereas they are far superior when the data are contaminated by outliers.

It should be noteworthy that the proposed robust  $X$ -bar charts based on the proposed methods in (5) and (11) rely on a key assumption that the underlying distribution is normally distributed, thus limiting their practical applications in statistical process monitoring, since this distribution is (almost always) unknown. A natural way to deal with the non-normality model departure issue is to adopt a certain type of data transformations to achieve approximate normality, whereas Khakifirooz et al. (2021) recently pointed out several dangers and pitfalls in the use of nonlinear transformations to obtain the approximate normality of the process data. In ongoing work, we continue to investigate the performance of the robust  $X$ -bar control charts when the underlying distribution exhibits departures from the normal distribution, such as skewed distributions.

Finally, it is noteworthy that we have developed `rcc()` function in `rQCC` R package (Park and Wang, 2022) to construct various robust control charts to help field engineers and practitioners to monitor the state of the process.



## References

- Abu-Shawiesh, M. O. A. (2008). A simple robust control chart based on mad. *Journal of Mathematics and Statistics*, 4:102–107.
- Alloway, Jr., J. A. and Raghavachari, M. (1991). Control chart based on the Hodges-Lehmann estimator. *Journal of Quality Technology*, 23(4):336–347.
- Burr, I. W. (1969). Control charts for measurements with varying sample sizes. *Journal of Quality Technology*, 1:163–167.
- Faraz, A., Saniga, E., and Montgomery, D. (2019). Percentile-based control chart design with an application to Shewhart  $\bar{X}$  and  $S^2$  control charts. *Quality and Reliability Engineering International*, 35(1):116–126.
- Fisher, R. A. (1922). On the mathematical foundations of theoretical statistics. *Philosophical Transactions of the Royal Society of London. Series A, Containing Papers of a Mathematical or Physical Character*, 222:309–368.
- Huber, P. J. and Ronchetti, E. M. (2009). *Robust Statistics*. John Wiley & Sons, New York, 2nd edition.
- Janacek, G. J. and Meikle, S. E. (1997). Control charts based on medians. *Journal of the Royal Statistical Society: Series D (The Statistician)*, 46(1):19–31.
- Khakifirooz, M., Tercero-Gómez, V. G., and Woodall, W. H. (2021). The role of the normal distribution in statistical process monitoring. *Quality Engineering*, 33(3):497–510.
- Kim, K. and Reynolds, Jr., M. R. (2005). Multivariate monitoring using an mewma control chart with unequal sample sizes. *Journal of Quality Technology*, 37(4):267–281.
- Kosztván, Z. T. and Katona, A. I. (2018). Risk-based X-bar chart with variable sample size and sampling interval. *Computers & Industrial Engineering*, 120:308–319.
- Lèvy-Leduc, C., Boistard, H., Moulines, E., Taqqu, M. S., and Reisen, V. A. (2011). Large sample behaviour of some well-known robust estimators under long-range dependence. *Statistics*, 45:59–71.
- Montgomery, D. C. (2013). *Statistical Quality Control: An Modern Introduction*. John Wiley & Sons, Singapore, 7th edition.

- Montgomery, D. C. (2019). *Introduction to Statistical Quality Control*. John Wiley & Sons, Singapore, 8th edition.
- Pappanastos, E. A. and Adams, B. M. (1996). Alternative designs of the Hodges-Lehmann control chart. *Journal of Quality Technology*, 28(2):213–223.
- Park, C. and Basu, A. (2011). Minimum disparity inference based on tangent disparities. *International Journal of Information and Management Sciences*, 22:1–25.
- Park, C., Kim, H., and Wang, M. (2022). Investigation of finite-sample properties of robust location and scale estimators. *Communication in Statistics – Simulation and Computation*, To appear.
- Park, C. and Leeds, M. (2016). A highly efficient robust design under data contamination. *Computers & Industrial Engineering*, 93:131–142.
- Park, C., Ouyang, L., Byun, J.-H., and Leeds, M. (2017). Robust design under normal model departure. *Computers & Industrial Engineering*, 113:206–220.
- Park, C., Ouyang, L., and Wang, M. (2021). Robust g-type quality control charts for monitoring nonconformities. *Computers & Industrial Engineering*, 162:107765.
- Park, C. and Wang, M. (2020). A study on the X-bar and S control charts with unequal sample sizes. *Mathematics*, 8(5):698.
- Park, C. and Wang, M. (2022). rQCC: Robust quality control chart. <https://CRAN.R-project.org/package=rQCC>. R package version 2.22.5 (published on May 23, 2022).
- Rocke, D. M. (1989). Robust control charts. *Technometrics*, 31(2):173–184.
- Serfling, R. J. (2011). Asymptotic relative efficiency in estimation. In Lovric, M., editor, *Encyclopedia of Statistical Science, Part I*, pages 68–82. Springer-Verlag, Berlin.
- Shewhart, W. A. (1926). Quality control charts. *Bell Systems Technical Journal*, 5:593–603.
- Vining, G. (2009). Technical advice: Phase I and Phase II control charts. *Quality Engineering*, 21(4):478–479.
- Wheeler, D. J. (2010). Are you sure we don't need normally distributed data? More about the misuses of probability theory. <https://www.qualitydigest.com/inside/six-sigmacolumn/are-you-sure-we-don-t-need-normally-distributed-data-110110.html>. Quality Digest.

Woodall, W. H. and Faltin, F. W. (2019). Rethinking control chart design and evaluation. *Quality Engineering*, 31(4):596–605.

Yao, Y. and Chakraborti, S. (2021). Phase I monitoring of individual normal data: Design and implementation. *Quality Engineering*, 33(3):443–456.